Spatial Metrics and Image Texture for Mapping Urban Land Use

Martin Herold, XiaoHang Liu, and Keith C. Clarke

Abstract

The arrival of new-generation, high-spatial-resolution satellite imagery (e.g., Ikonos) has opened up new opportunities for detailed mapping and analysis of urban land use. Drawing on the traditional approach used in aerial photointerpretation, this study investigates an "object-oriented" method to classify a large urban area into detailed land-use categories. Spatial metrics and texture measures are used to describe the spatial characteristics of land-cover objects within each land-use region as derived from interpreted aerial photographs. In assessing how land-use categories vary in their spatial configuration, spatial metrics were found to provide the most important information for differentiating urban land uses. A detailed land-use map with nine categories was derived for the Santa Barbara South Coast Region area. Results from our work suggest that the region-based method exploiting spatial metrics and texture measurements is a potential new avenue to extract detailed urban land-use information from high-resolution satellite imagery.

Introduction

Detailed information on urban land use is essential for applications related to urban management and planning (Jensen and Cowen, 1999). For decades, large-scale air photos have been employed to obtain such information by applying the principles of aerial photointerpretation. Interpretation using texture, context, and spatial configurations of urban land-cover features are well documented (Bowden *et al.*, 1975; Haack *et al.*, 1977; McKeown, 1988). The availability of very-high-spatial-resolution satellite imagery offers a new avenue to obtain urban information on a very detailed level (Welch, 1982; Donnay *et al.*, 2001; Small, 2001). Traditional human approaches followed the hierarchical relationships of the basic image interpretation elements shown in Figure 1. Tone and color are of fundamental importance and represent primary image elements. For digital data this primary feature is given by the spectral information (on a per-pixel basis) and characterizes the land-cover type of a specific surface object such as a vegetated zone or a built-up area. The spatial arrangement and configuration of the basic elements represent interpretation features of greater complexity such as size, shape and texture, or pattern and association. Higher elements of interpretation usually improve the level of detail and accuracy that can be derived from the remote sensing datasets. Their application, however, commonly requires higher level efforts in the image analysis processes in terms of more sophisticated knowledge of the human interpreter or more complex and customized digital image processing algorithms (Haack *et al.*, 1997).

Although an experienced image interpreter can utilize image elements well in visual interpretation, the expert knowledge is not easily translated to the analysis of satellite imagery. To explore the rich dataset provided by Ikonos or QuickBird, a bridge needs to be built between the well-established approaches of visual interpretation and digital image processing. A key issue is to explore and evaluate the quantitative descriptors of spatial urban form to find distinct relationships between the physical spectral measurement (of radiance) and the land-use, socio-economic, demographic, and ecological characteristics of individual land-cover objects.

Techniques for including spatial, textural, and contextual information in digital mapping of urban areas from remotely sensed imagery have been developed and tested in the last three decades (Gong *et al.*, 1992; Barnsley *et al.*, 1993). The approaches vary in terms of their image base (continuous spectral image or discrete land-cover classification), the spatial analysis domain (kernel-based or region-based), and the statistical approach used in describing the spatial and textural components. In the domain of high spatial resolution remote sensing, image analysis has to consider the specific characteristics and limitations of the data for depicting the urban environment. The incorporation of higher order image interpretation elements such as shape and size of land-cover objects requires a clear representation of these characteristics in the remotely sensed imagery. For urban areas, spatial resolutions of better than five meters are usually required for the identification of land-cover objects such as buildings (Welch, 1982; Jensen and Cowen, 1999).

The hierarchy of urban image objects (Haack *et al.*, 1997; Zhan *et al.*, 2002) represents the urban landscape as "land-cover objects" and "land-use regions" (or objects). Land-use regions are comprised of land-cover objects, e.g., a block (land-use object) consisting of several buildings and vegetated areas (land-cover objects). In contrast to natural environments, man-made structures have been identified as one of the few examples of objects within a landscape that have distinct and crisp boundaries (Couclelis, 1992). This characteristic makes the general approach particularly suitable in urban analysis.

Recent developments in "object-oriented" image classification (based on image segmentation) have taken advantage of the detailed spatial characteristics of high-resolution datasets. The research in this area has emphasized the reduction of spectral variability within the objects and the incorporation of additional information from spatial and contextual image/object characteristics (Johnsson, 1994; Blaschke and Strobl, 2001). Land-use regions or objects follow the concept of "analytical areas" and "photomorphic areas or units" (Peplies, 1974; Haack *et al.*, 1997). This concept of regionalization was developed and is commonly used for aerial photographic interpretation and mapping. Land-use regions are defined as

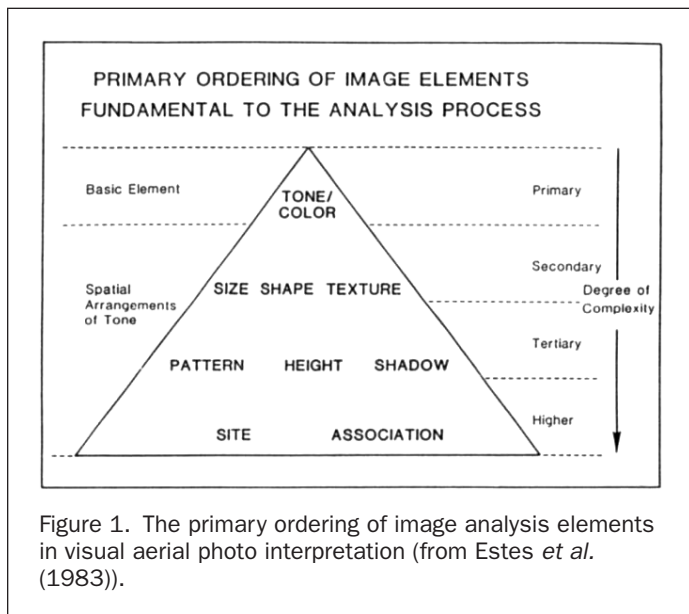Department of Geography, University of California Santa Barbara, Santa Barbara, CA 93106 (martin@geog.ucsb.edu).

Figure 1. The primary ordering of image analysis elements in visual aerial photo interpretation (from Estes *et al.* (1983)).

shape and spatial arrangement (Moller-Jensen, 1990; Barnsley and Barr, 1997) usually referred to as "urban morphology" (Webster, 1995, p. 280). In that context, the use of spatial metrics has provided a new avenue for describing the spatial land-cover heterogeneity and morphological characteristics within the urban environment. As landscape metrics, spatial metrics are already commonly used to quantify the shape and pattern of quasi-natural vegetation in natural landscapes (O'Neill *et al.*, 1988; Gustafson, 1998; McGarigal *et al.*, 2002). Recently, there has been an increasing interest in applying spatial metric techniques in an urban environment to link land-cover heterogeneity to structures and dynamic changes in urban land uses (Herold *et al.*, 2002a).

The research presented here provides an evaluation of texture measurements and spatial metrics as quantitative discriminators of urban spatial characteristics for the mapping of urban land uses. The analysis is based on a mosaic of seven multispectral Ikonos images that cover the whole urban area in the Santa Barbara South Coast Region, California. Given the size and heterogeneity of the study area, this study contains considerable variability within urban land-use classes and is not limited to specific unique small test sites. The study is part of the UCIME project (UCIME, 2001), which in part aims to identify innovative data sources to describe urban morphology and provide useful information for managers and planners.

Study Area
The focus of the study is the urbanized area of the south coast region in Santa Barbara County, California. The South Coast Region is located about 170 kilometers northwest of Los Angeles in the foothills of the Santa Ynez Coast Range (Figure 2) with a size of about 300 sq km and a total population of around 200,000 people. The area consists of different types of land use, including residential areas with different density and socio-economic structure; mixed-use areas (e.g., downtown areas); and commercial and industrial districts with various urban built-up cover types like roofs, roads, parking lots, sidewalks, recreational areas, and others.

Processing of Ikonos Data
Remotely sensed imagery covering the study area was acquired from the University of California Santa Barbara Map and Image Laboratory (UCSB/MIL). The main dataset is comprised of seven individual multispectral Ikonos images (4-m spatial resolution) acquired between March and July 2001 covering the

spatially distinct areas with homogeneous structure that are composed of an aggregation of land-cover objects representing a specific type of land use (Moller-Jensen, 1990; Aplin *et al.*, 1999; Herold *et al.*, 2002a; Zhan *et al.*, 2002). Given this background, it is argued that the analysis of high-spatial-resolution remote sensing data in the urban environment has to consider an "object-oriented" approach. Common techniques using artificial image structures such as pixels or a moving kernel window should be reconsidered because object-based methods focus on the analysis of thematically defined, irregularly shaped objects and regions.

There are several approaches describing the spatial, textural, and contextual characteristics of urban land-cover objects. Texture parameters based on the co-occurrence matrix (Haralick, 1973) have shown the capability of capturing the land-use variation within an urban environment (Baraldi and Parmiggiani, 1995; Liu and Clarke, 2002). Other second-order image interpretation elements in Figure 1 were also studied. Related research has focused on the analysis on image-derived objects such as buildings and roads, and tried to describe their
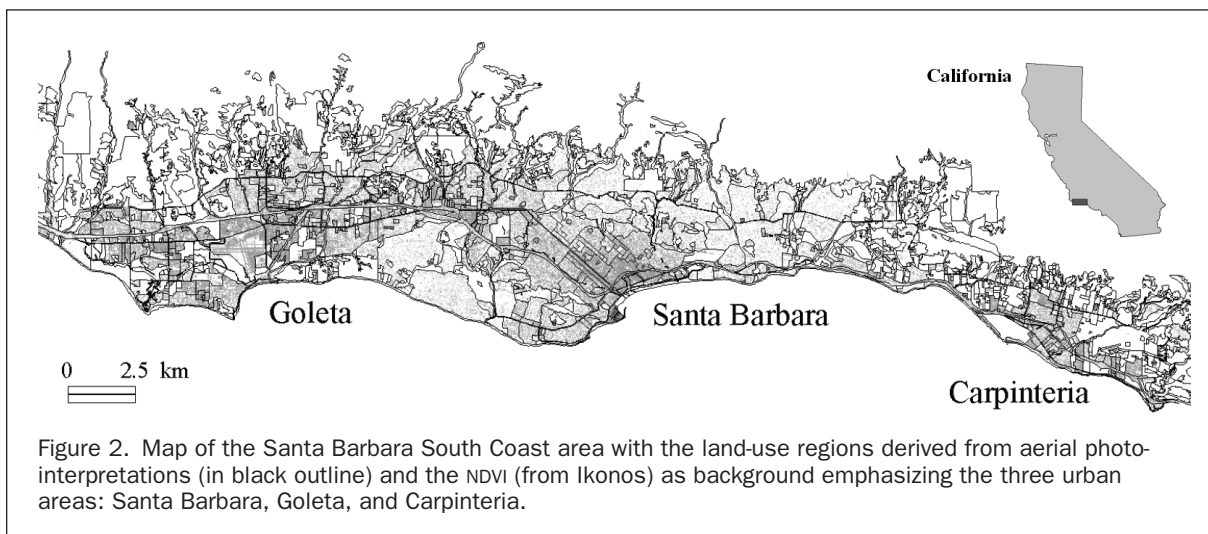

Figure 2. Map of the Santa Barbara South Coast area with the land-use regions derived from aerial photo-interpretations (in black outline) and the NDVI (from Ikonos) as background emphasizing the three urban areas: Santa Barbara, Goleta, and Carpinteria.

TABLE 1. ERROR MATRIX OF LAND-COVER CLASSIFICATION USING IKONOS IMAGE

Class	Green Veg	Building	Rest	# of Samples	Producer Accuracy
Green vegetation	103	8	12	123	83.7
Buildings/Roofs	0	278	58	336	82.7
Rest	5	57	276	338	81.7
Total	108	343	346	797	
User accuracy	95.4	81.0	79.8		**Overall: 82.4 %**

Santa Barbara urban area (Figure 2). The data were acquired on different dates with varying atmospheric and illumination conditions. Geometric rectification (polynomial image-to-image registration) and atmospheric corrections (empirical line method) were accomplished with standard image analysis algorithms, resulting in an accurate and normalized image mosaic (Herold *et al.*, 2002b). An object-oriented land-cover classification was performed in eCognition software (Baatz *et al.*, 2001) using all four spectral bands. ECognition uses image segmentation to homogenize the spectral variability within land-cover segments and perform the classification based on those objects. The software allows for the incorporation of spatial and contextual information of object features in the image classification process (Baatz *et al.*, 2001). Given the purpose of this research, the image classification focused on the derivation of three major land-cover classes: buildings, green vegetation, and the rest, including roads, parking lots, bare soil, water bodies, and non-photosynthetic vegetation.

Green vegetation spectrally separates fairly well. However, there are some spectral similarities between buildings or roof types and other urban targets such as roads and bare soil surfaces, especially given the relatively low spectral resolution of Ikonos (Herold *et al.*, 2003). To solve this problem, additional spatial information was included in the classification process to improve the land-cover map. The object length/width ratio was used to separate buildings (compact quadratic/rectangular) from roads (linear). A minimum-object-size rule was applied to overcome spectral confusion between specific roof types and bare soil surfaces. The accuracy of the land-cover classification is shown in Table 1. The error matrix was determined by random sampling of test-object areas and shows overall good classification results of 82.4 percent overall accuracy. Green vegetation is mapped with the highest accuracy, with a tendency to be overmapped. There is still some confusion between the buildings/roofs and the other land-cover classes due to the aforementioned spectral similarity. This problem was not completely resolved by including spatial object information. Detailed information on the pre-processing and image classification of the Ikonos data is documented in Herold *et al.* (2002b).

Derivation of Land-Use Regions
Different ways of spatially subdividing an urban area have been proposed based on administrative boundaries, remote sensing and/or map analysis, and urban modeling approaches. A common approach is to use a quadratic window or kernel to analyze the features in the neighborhood of a pixel. Barnsley and Barr (2000) discussed several problems related to kernel-based approaches in urban analysis. For example, grid-based approaches tend to smooth the boundaries between discrete land-cover/land-use parcels; it is difficult to determine *a priori* the optimum kernel size; and, a rectangular window represents an artificial area that does not conform to real parcels or land-use units, which tend to have irregular shapes and their own distinct spatial boundaries. In contrast, region-based approaches allow a discrete characterization of thematically and

functionally defined areas that are generally irregularly shaped (Gong *et al.*, 1992; Barnsley and Barr, 2000).

Regional subdivisions of urban space exhibit considerable variation in size, shape, and purpose. Governmental and planning organizations use census tracts or zoning districts which are designed according to the characteristics of the built environment, socioeconomic variables, administrative boundaries, and other considerations (Knox, 1994). Urban GIS and models have also used a wide variety of spatial units, including individual parcels as the spatial representations of land ownership, and uniform analysis zones defined by the intersections of multiple data layers. Automated techniques are usually based on pattern recognition or image segmentation that provides areas with similar spectral and textural pattern (Zhan *et al.*, 2002). In contrast, traditional visual interpretation approaches in region-based remote sensing analysis follow the concepts of "analytical areas" or "photomorphic units and regions" (Peplies, 1974; Haack *et al.*, 1997). This approach is used in this study. Although the air photo derived regions provide a suitable set of land-use zones, the approach requires additional work in delineating these areas.

The land-use regions for the whole study area were delineated by an experienced image analyst using 6-foot (1.8 m) resolution aerial photographs acquired in 1998 (see Figure 2). The regions represent areas with homogeneous land-cover characteristics according to their tone/color, the size and shape of land-cover objects, and their texture and pattern (Peplies, 1974; Haack *et al.*, 1997). Due to the temporal differences between the air photos and the Ikonos image acquisition, the areas were inspected for their accuracy. In areas of urban growth and land-use change, specific regions had to be modified and adjusted. Although each region is attributed with a land-use category, this study only used the spatial outline, hence geometry, of the regions and not the attribute information. All selections and interpretations of land-use training and test regions were based on maps and field observations. Regions smaller than 1 acre (0.4 ha) were excluded from the analysis, because they are too small given the scale of the analysis. In all, over 1700 land-use regions were incorporated in the investigation.

Derivation and Analysis of Texture and Spatial Metrics
Texture and spatial metrics were derived for each land-use region. For texture calculation, the near-infrared band of Ikonos imagery was used, which carries the most significant amount of information in terms of vegetation versus built-up land-cover types. While there are several methods to calculate image texture, this research uses the Gray-level Co-occurrence matrix (GLCM) to describe image texture. GLCM is an approximation of the joint probabilistic density function of pixel pairs and is fairly insensitive to abnormal values. GLCM is suitable to describe the texture of land-use regions with irregular shape such as those in this study. A displacement of five pixels in an omni-directional setting was used for GLCM calculation. The five-pixel distance corresponds to 20 meters on the ground. This approximately represents the average distance between urban land-cover objects as identified by the spatial autocorrelation analysis (Small, 2001). Seven commonly used texture descriptors were examined, including energy, entropy, contrast, correlation, variance, dissimilarity, and homogeneity. The statistical definitions of these descriptors are listed in Table 2 together with a brief description of their meanings. For a detailed discussion, readers are directed to Haralick (1973) and Baraldi and Parmiggiani (1995).

While texture measurement is based on continuous gray-level pixel values, the calculation of spatial metrics is based on a categorical, patch-based representation of the landscape within individual land-use regions. In general, patches are

TABLE 2. DESCRIPTION OF THE TEXTURE PARAMETERS

Texture Descriptor	Description
Energy $= g(i, j)$	Measures texture uniformity, or pixel pair repetitions. High energy occurs when the distribution of gray level values is constant or period.
Entropy $= \sum_{i=0}^{N_g-1} \sum_{j=0}^{N_g-1} g^2(i, j)\log(g(i, j))$	Highly correlated to energy. Measures the disorder of an image. Entropy is high when an image is not texturally uniform.
Contrast $= \sum_{i=0}^{N_g-1} \sum_{j=0}^{N_g-1} (i - j)^2 g^2(i, j)$	Contrast measures the difference between the highest and lowest values of a contiguous set of pixels. Low contrast image features low spatial frequencies.
Variance $= \sum_{i=0}^{N_g-1} \sum_{j=0}^{N_g-1} (i - u)^2 g(i, j)$	A measure of heterogeneity. Variance increases when the gray level values differ from their mean.
Dissimilarity $= \sum_{i=0}^{N-1} \sum_{j=0}^{N-1} g(i, j)|i - j|$	The dissimilarity is similar to Contrast. Instead of weighting the diagonal exponentially, the dissimilarity weights increase linearly.
Homogeneity $= \sum_{i=0}^{N_g-1} \sum_{j=0}^{N_g-1} \frac{1}{1+(i - j)^2} \cdot g(i, j)$	Measure image homogeneity. Sensitive to the presence of near diagonal elements in a GLCM.

where N_g is the number of gray levels, entry (i, j) in the Gray Level Co-occurrence Matrix and

$$u = \sum_{i=0}^{N_g-1} \sum_{j=0}^{N_g-1} i.g(i, j) \qquad \text{and} \qquad \sigma^2 = \sum_{i=0}^{N_g-1} \sum_{j=0}^{N_g-1} (i - u)^2 g(i, j).$$

defined as homogeneous regions for a specific landscape property of interest such as "building" or "vegetation." This landscape perspective assumes abrupt transitions between individual patches that result in distinct edges. Spatial metrics can be used to quantify the spatial heterogeneity of the individual patches, all patches in the same class, and the landscape as a collection of patches. Some metrics are spatially non-explicit scalar values, but still capture important spatial properties. Spatially explicit metrics can be computed as patch-based indices (e.g., size, shape, edge length, patch density, fractal dimension) or as pixel-based indices (e.g., contagion) computed for all pixels in a patch (Gustafson, 1998; McGarical et al., 2002). The data set used to calculate the spatial metrics is the classified Ikonos imagery, consisting of three land-cover types: building, vegetation, and the rest. Metrics calculations are performed on the building and vegetation classes only, using the public domain software FRAGSTATS Version 3.3 (McGarical et al., 2002).

Table 3 describes the spatial metrics used in this research. A more detailed description, including the specific mathematical equations of all of the metrics, can be found in McGarical et al. (2002). The selection of the metrics was based on their value in quantifying specific landscape characteristics that have been identified in previous research on urban areas (Herold et al., 2002a). Most metrics have fairly simple and intuitive values such as the percentage of the landscape covered by the class (PLAND), the patch density (PD), the mean patch size (AREA_MN) and standard deviation (AREA_SD), and the measures of mean Euclidean distance (ENN_MN) and standard deviation (ENN_SD). The largest patch index (LPI) metric describes the percentage of the total area covered by the class concentrated in the largest patch of that class. The contagion index (CONTAG) measures to what extent landscapes are aggregated or clumped (O'Neill et al., 1988). Landscapes consisting of relatively large, contiguous patches are described by a high contagion index. If a landscape is dominated by a relatively greater number of small or highly fragmented patches, the contagion index is low. The fractal dimension describes the complexity and the fragmentation of a patch by a perimeter-area proportion. Low values are derived when a patch has a compact rectangular form with a relatively small perimeter relative to the area. If the patches are more complex and fragmented,

the perimeter increases and yields a higher fractal dimension. The fractal dimension was calculated as the area weighted mean patch fractal dimension (FRAC_AM) and fractal dimension standard deviation (FRAC_SD). FRAC_AM averages the fractal dimensions of all patches by higher weighting of larger land-cover patches. The shape of smaller patches is often determined more by image pixel size than by characteristics of natural or manmade features. The patch Cohesion measures the physical connectedness of the corresponding land-cover class. The cohesion increases as the patches that comprise a class become more clumped or aggregated in the class distribution, hence is more physically connected (Gustafson, 1998). Overall, 22 metrics were included in the further analysis. The Contagion metric describes the whole landscape considering all patches of all classes (buildings and vegetation). Eleven metrics were derived for the class "buildings," e.g., considering all building patches or objects within a land-use region. All of them are described in Table 3. The same class metrics have been used for describing the class "vegetation," except for the LPI measure, which was excluded after correlation analysis.

The seven texture parameters and 22 metrics were calculated for each of the land-use regions in the study area. This produced a 29-dimensional attribute vector for each region. To study the separability between different land-use classes using the attribute vector, Bhattacharyya distance (B-distance) was calculated to assess the contribution of each metric for the land-use discrimination. The Fisher Linear Discriminant algorithm is used to classify each land-use region into a land-use class. Both algorithms are implemented in the public domain program MULTISPEC. This program was designed for the processing and analysis of hyper-dimensional datasets (Landgrebe and Biehl, 2001) and was applied in this study. The Bhattacharyya distance (B-distance) is a commonly used measure of statistical distance between two Gaussian distributions (Kailath, 1967) and incorporates both first-order (mean) and second-order (covariance) statistics. The separability analysis was performed based on the training dataset that is described in the next section. A more detailed analysis of the individual contributions of the mean and covariance component of the B-distance has shown that the mean difference contributes most of the discrimination between

TABLE 3. DESCRIPTION OF THE SPATIAL METRICS

Metric	Description/Calculation Scheme	Units	Range
PLAND - Percentage of landscape	PLAND equals the sum of the areas (m²) of a specific land cover class divided by total landscape area, multiplied by 100.	Percent	$0 < PLAND \leq 100$
PD - Patch density	PD equals the number of patches of a specific land cover class divided by total landscape area.	Numbers per 100 ha	$PD \geq 1$, no limit.
AREA_MN - Mean patch size	AREA_MN equals the average size of the patches of a land cover class.	Hectares	$AREA\_MN \geq 0$, no limit.
AREA_SD - Area standard deviation	AREA_SD equals the standard deviation in size of the patches of a land cover class.	Hectares	$AREA\_SD \geq 0$, no limit.
ED - Edge density	ED equals the sum of the lengths (m) of all edge segments involving a specific class, divided by the total landscape area (m²) multiplied by 10000 (to convert to hectares).	Meters per hectare	$ED \geq 0$, no limit.
LPI - Largest patch index	LPI equals the area (m²) of the largest patch of the corresponding class divided by total area covered by that class (m²), multiplied by 100 (to convert to a percentage).	Percent	$0 < LPI \leq 100$
ENN_MN - Euclidian mean nearest neighbor distance	ENN_MN equals the distance (m) mean value over all patches of a class to the nearest neighboring patch based on shortest edge-to-edge distance from cell center to cell center.	Meters	$ENN\_MN > 0$, no limit.
ENN_SD - Euclidian nearest neighbor distance standard deviation	ENN_SD equals the standard deviation in euclidian mean nearest neighbor distance of land cover class.	Meters	$ENN\_SD > 0$, no limit.
FRAC-AM - Area weighted mean patch fractal dimension	Area weighted mean value of the fractal dimension values of all patches of a land cover class, the fractal dimension of a patch equals 2 times the logarithm of patch perimeter (m) divided by the logarithm of patch area (m²); the perimeter is adjusted to correct for the raster bias in perimeter.	None	$1 \leq FRAC\_AM \leq 2$
FRAC-SD - Fractal dimension standard deviation	FRAC_SD equals the standard deviation in fractal dimension of land cover class.	None	$FRAC\_SD > 0$, no limit.
COHESION	Cohesion is proportional to the area-weighted mean perimeter-area ratio divided by the area-weighted mean patch shape index (i.e., standardized perimeter-area ratio).	Percent	$0 < COHESION < 100$
CONTAG - Contagion	CONTAG measures the overall probability that a cell of a patch type is adjacent to cells of the same type.	Percent	$0 < CONTAG \leq 100$

the land-use categories. The main reason for applying the B-distance for this study is the large dynamic range with no saturation value like other separability measures such as the Transformed Divergence or Jeffreys-Matusita distance (Mausel *et al.*, 1990). Another advantage of using the B-distance is that the individual B-distance scores can be aggregated to identify the texture parameters and metrics that contribute the most in discrimination of the land-use classes. This algorithm is commonly used for band prioritization in hyperspectral image analysis and is implemented in MULTISPEC.

The land-use classification was conducted using the Fisher Linear Discriminant (FLD) algorithm with the metrics and texture descriptors. FDL is a supervised classification approach that projects the original hyper-dimensional dataset to a lower dimensional space where the distance between classes in the new space is maximized and the distance between members within each class is minimized (Klecka, 1980). The classification is then performed in the one-dimensional domain. This algorithm was chosen because of the large number and variability of texture and spatial measures and the limited number of training samples for each class (described in the next section). The actual classification used the training areas for calibration. Three classifications have been performed: using the 22 spatial metrics, using the six texture parameters, and using the combination of the two.

Urban Land-Use Characteristics

The investigations considered nine different urban land-use categories. Given the extent of the study area, the definition of the classes had to represent the whole land-use variability

within the Santa Barbara South Coast region. The nine categories are described in Table 4. The table emphasizes the number of training samples and test samples that were used in the analysis, hence the separability assessment and the classification. Visual examples of the spatial land-cover structure of the major urban land-use classes are presented in Figure 3. Most of the urbanized area is comprised of single unit residential homes with different density and socioeconomic structure. Population density measures that have been estimated for each of the regions using U.S. Census data (Liu and Clarke, 2002) were incorporated as additional indicators in the interpretation analyses if the visual spatial pattern did not resolve a clear distinction between low, medium, and high density residential.

Figure 3 emphasizes the specific differences in spatial urban morphology between the different urban land-use categories. Important features are the sizes of buildings, their shape, and their spatial configuration. For example, areas of low, medium, and high-density residential land use represent a spatial built up structure ranging from a detached irregular structure to the regular high-density arrangement of buildings of the typical American block pattern. Commercial/industrial and institutional land uses indicate significantly larger buildings and a more aggregated spatial configuration. The spatial structures are also reflected by the spatial heterogeneity of the vegetated areas. The vegetation patches vary in terms of their spatial extent and fragmentation. Vegetation represents a somewhat inverse pattern of the building structure. These variations are important because they indicate that both the vegetation and building spatial patterns contribute to the characterization of urban morphology.

TABLE 4. DEFINITION OF LAND-USE CLASSES

Land Use Class	Description and Characteristics	# of Training Areas	# of Test Areas
Low density single unit residential	Low density detached housing, high income areas with low population density, large buildings with irregular spatial arrangement, large parcel size with dominant vegetation land cover	23	39
Medium density single unit residential	Medium density housing, areas with medium population density, average too large residential buildings and some degree of distinct spatial arrangements along roads, landscape dominated by vegetation cover	22	30
High density single unit residential	High density low income housing, small homogenous building units with distinct regular spatial structure and small and fragmented intermediate vegetation patches	33	41
Multi unit residential	Residential areas with multiple unit or multi-family housing and mixed residential land uses including condos, apartment buildings etc., large building units with regular shape and distinct spatial arrangement, large intermediate vegetated areas	29	34
Commercial and Industrial	Large regular commercial and industrial building structures, sometimes in combination residential housing, high degree of imperviousness and only few small fragmented vegetation patches	32	43
Institution	Educational and research institutions, churches and other distinct religious buildings, and hospitals, large spatially clumped building structures surrounded by large vegetated areas	20	22
Recreational and open spaces	Parks, open urban space, vacant lots and other recreational facilities such as golf courses, soccer and baseball fields etc., dominated by vegetation and non-impervious cover types, sporadic isolated buildings	24	23
Agriculture and rangeland	Areas with intensive and extensive agriculture (field crops, orchards, vineyards) and livestock (cattle), dominated by vegetated surface types with distinct spatial cultivation pattern	37	45
Forest and wetlands	Natural or quasi-natural, uncultivated areas including protected areas and riparian zones, dominated by tree and natural vegetation with indistinct spatial pattern	22	28

Figure 3 also highlights some of the inaccuracies in the classification process. Confusion exists between buildings and roads. However, given the accuracies in Table 1, the general spatial landscape structures are clearly represented by the classification result and were considered suitable for further investigation.

The number of training and test areas used for the classification is presented in Table 4. The training areas were selected from representative regions in each land-use category through visual image interpretations and ground observations. The training data were used for the separability analysis based on B-distance and the calibration of the supervised classification. The test regions were used to assess the accuracy of the final classification. To provide a statistically rigorous and robust evaluation of the mapping product, test regions were randomly selected from all land-use regions and were interpreted or inspected on the ground. Additional samples of recreation/open space and institutions were added so that each class has a minimum of 20 test regions.
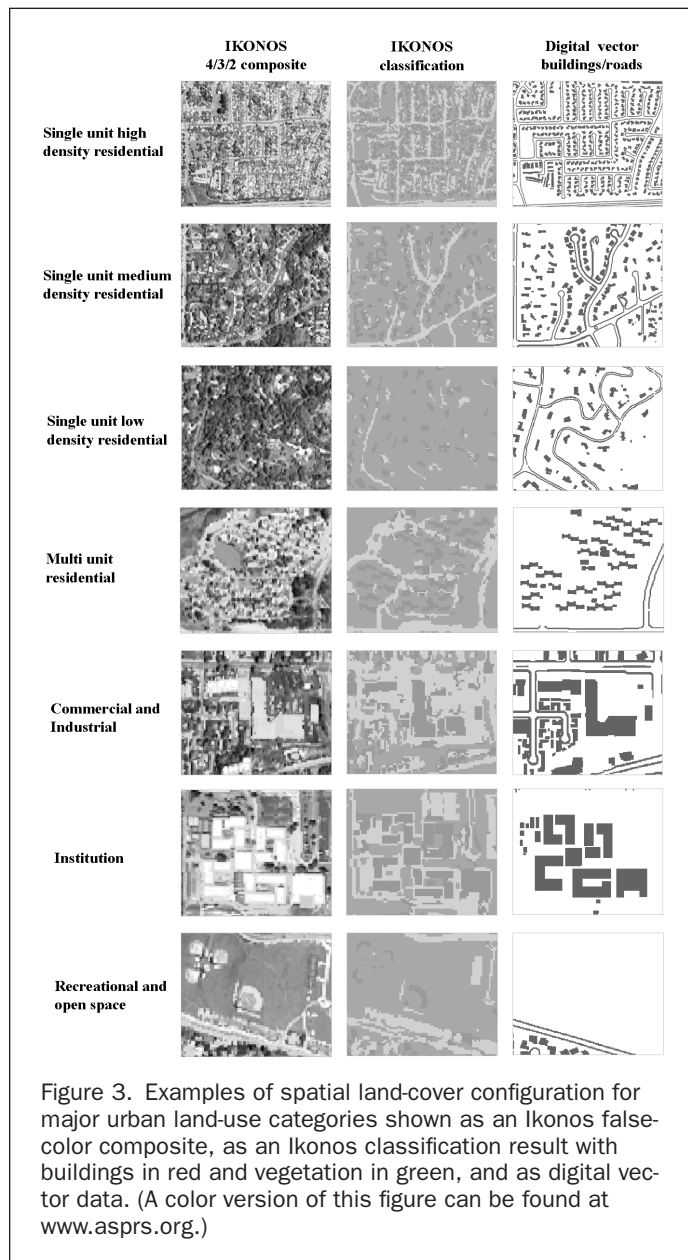
Results and Discussion

Urban Land-Use Separability

The B-distance separability scores between individual land-use classes are shown in Table 5. The scores are derived from the training regions and all 29 texture and metric measurements. The values range from 6.5 to 64.9, indicating that the categories do separate. Some scores, however, seem comparatively low. There is some confusion between residential classes, e.g., low versus medium density single unit and between medium/high density residential and multi-unit residential. These confusions were expected because all residential classes consist of similar land-cover types, e.g., buildings and vegetation. High-density residential and commercial classes show some degree of similarity. They are known to have a similar degree of imperviousness and, if commercial

uses are combined with residential housing, the pattern is expected to appear similar in most of the textures and metrics. Institutions, multi-unit residential, and commercial/industrial sometimes share a similar spatial pattern of large, compact houses, resulting in comparatively low B-distance scores. The land-use types dominated by vegetation also indicate a relatively low separability, e.g., between agriculture, forest, and low-density residential housing.

Assessment of Most Suitable Texture and Spatial Metrics

As discussed previously, the individual B-distance scores presented in Table 5 can be aggregated over all classes to identify the combination of texture parameters and metrics that contribute the most discrimination between different land-use categories. The calculation was focused on a set of six measurements of 29 texture/metrics overall. This "most suitable" set of metric or texture parameters represents the set that provides either the best average or best minimum separability for all classes. The analysis was done for two sets of land classes: including all nine categories and for only the built up land-use types (excluding agriculture and forest) to emphasize the focus of this study on spatial urban morphology. To provide a "suitability" score for each texture or metric, the top five ranking sets of six measures (metric or texture) were calculated and considered in the interpretation. The next ranked sets of optimal texture/metric combinations only showed minor differences in their determining B-distance scores compared to the top ranked combination. The analysis required four calculations, given two sets of categories (all nine and just seven built up) and consideration of the best minimum and average separability for both of them. Each calculation provided the five most suitable combinations of six metric/texture, i.e., each measure has a theoretical chance to be chosen a maximum of 20 times. The frequency of each individual texture or metric appearing in this analysis is considered the suitability score. The more often a metric/texture is determined to be

Figure 3. Examples of spatial land-cover configuration for major urban land-use categories shown as an Ikonos false-color composite, as an Ikonos classification result with buildings in red and vegetation in green, and as digital vector data. (A color version of this figure can be found at www.asprs.org.)

ple, the percentage of area covered by vegetation (PLAND) received a score of 16. These "most suitable" metric/texture measures are most informative in differentiating the land-use types within a region. In terms of vegetation land cover, patch size (AREA_MN) and its standard deviation (AREA_SD) are contributions, as well as COHESION, which describes the degree of spatial clustering. The spatial building structure of the land-use categories are most distinctively characterized by the average distance between the buildings (ENN_MN_U) and their standard deviation (ENN_SD_U). In areas where buildings display similar pattern, the distance between two adjacent buildings (ENN_MN_U) tends to be regular and thus has a small standard deviation (ENN_SD_U). The percentage of built up land (PLAND_U) and the largest patch index (LPI_U) describe the concentration of built-up area in a land-use region. The spatial fragmentation or heterogeneity of the buildings (ED_U) provides further important information in discriminating urban land use. CONTAGION is a measure of the heterogeneity of the overall urban landscape and appears as a suitable metric also. HOMOGENEITY is considered an important texture parameter because it contributes to the separation of all categories. It also has high suitability for the minimum separability of the built-up land use.

In general, the spatial metrics and texture descriptors that contribute best to the average separability provide a good overall contribution in discriminating all land-use types. In contrast, the minimum separability is associated with the classes with low separation, and Figure 4 highlights the bands that provide the largest amount of information for that purpose. Given this, it is obvious that the vegetation related metrics have their highest contribution for best average separability. The metrics describing housing structure and texture parameters appear more often for best minimum separability. Accordingly, the spatial structure and configuration of the vegetation patches are the most important and distinct level of information for general urban land-use discrimination. Although this result is evident, it might be somewhat biased by the fact that vegetation has a higher accuracy in the land-cover classification. Inaccuracies in the mapped building class might be reflected in metrics in a way that distorts distinct differences between the land-use types. Figure 4 further indicates that the spatial metrics are the major contributor for land-use separability. However, the texture measurements do appear to have an effect and add an additional level of information. It should be noted that the texture measurements were calculated using the near-infrared band of Ikonos only. A multi-band texture analysis with different lag-distances might improve the separability. The results in Figure 4 also emphasize that spatial structure and configuration of the land-cover classes provide more distinct information than the simple area coverage measure (PLAND and PLAND_U) alone. Simple area measures are quite often used as a discriminator for urban land-use characterization. In fact, a detailed classification of urban land use requires the information about the spatial land-cover structure and related high-spatial resolution

most suitable, the higher the contribution in separation of the urban land-use classes or the spatial land-cover pattern that characterizes them.

The results of the assessment of most suitable texture and spatial measurements are presented in Figure 4. The graph indicates some measurements with very high scores. For exam-
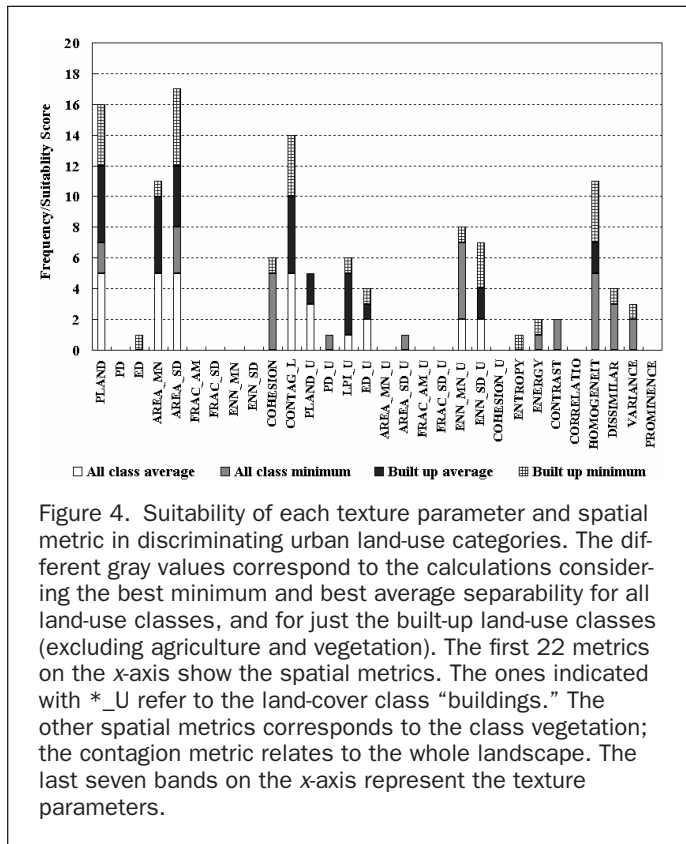
TABLE 5. B-DISTANCE SEPARABILITY MATRIX BETWEEN THE INDIVIDUAL LAND-USE CLASSES (VALUES LESS THAN 15 ARE HIGHLIGHTED IN BOLD)

Class	1: low_d	2: med_d	3: high_d	4: multi	5: institut	6: recreat	7: com	8: agri	9: forest
1: low_dens_res		**12.3**	25.4	19.7	22.1	21.4	27.8	**14.3**	20.4
2: med_dens_res			**15.3**	**13.3**	18.7	31.6	18.6	24.1	36.9
3: high_dens_res				**6.5**	**12.3**	50.9	**9.2**	38.5	64.6
4: multi_unit_res					**8.8**	27.4	**6.7**	23.4	53.9
5: institution						22.4	**9.1**	22.1	44.2
6: recreation_open							24.6	**7.8**	**13.9**
7: commerc_ind								24.4	48.6
8: agric_range									**7.2**
9: forest_wetland									

Figure 4. Suitability of each texture parameter and spatial metric in discriminating urban land-use categories. The different gray values correspond to the calculations considering the best minimum and best average separability for all land-use classes, and for just the built-up land-use classes (excluding agriculture and vegetation). The first 22 metrics on the *x*-axis show the spatial metrics. The ones indicated with *_U refer to the land-cover class "buildings." The other spatial metrics corresponds to the class vegetation; the contagion metric relates to the whole landscape. The last seven bands on the *x*-axis represent the texture parameters.

data that represents these surface properties with sufficient accuracy.

Land-Use Classification

The final step of the study was to classify all 1700 regions into urban land-use categories based on spatial metrics, texture parameters, and a combination of the two. The error matrix of the classification using all measures derived from the test areas is shown in Table 6. An overall accuracy of 76.4 percent and a Kappa coefficient of 73.4 percent indicate that the overall classification is good. Classes with a producer's accuracy above 85 percent are low density residential and institutions. Most categories have a producer's accuracy between 73 and 78 percent with agriculture and rangeland showing the lowest value of 62.2 percent. In terms of user's accuracy, commercial/industrial and low density residential seem to be most accurately mapped

while medium density residential, recreation/open space, and multi-unit residential are overmapped. The overall accuracy is relatively low. However, it must be stressed that the classification performed in this study is based on metrics and texture information only. Classes such us agriculture and forest (which happen to have low accuracy) can usually be easily differentiated using the spectral information of multiple bands. If color and tone information is incorporated, the classification accuracy is expected to improve further.
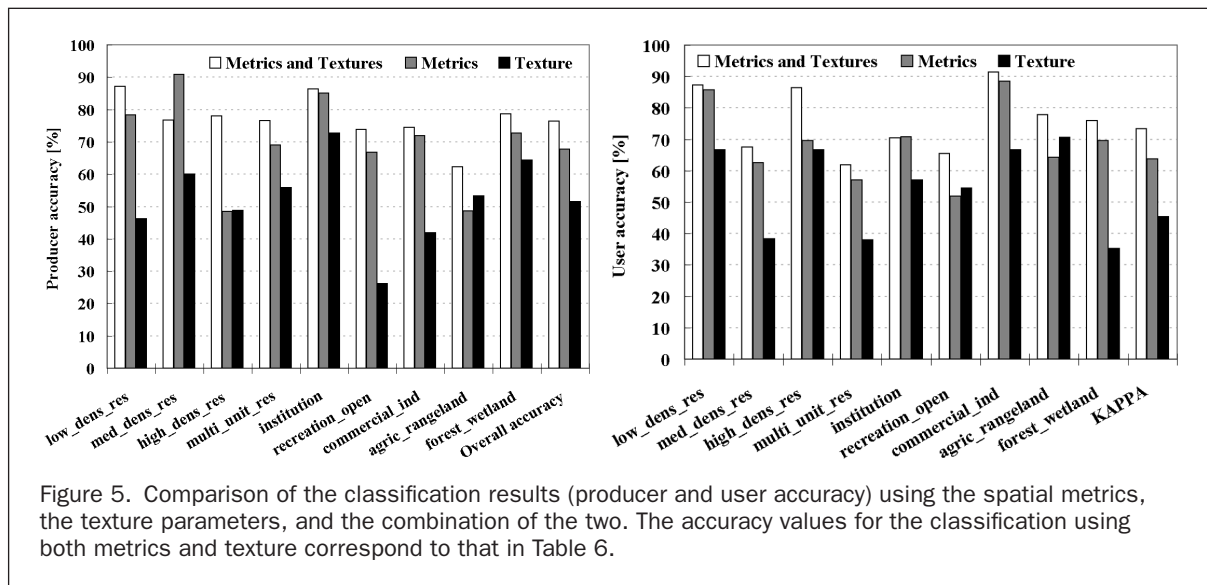
The confusion between different land-use classes echoes the separability matrix presented in Table 5. Most misclassifications of residential land uses happen among residential classes, except that some confusion exists between multi-unit residential and commercial/industrial use. Low density mixes with medium density residential and high density residential confuses with medium density and multi-unit residential. The other group of major confusion appears for the land uses that are dominated by vegetation, i.e., between recreation/open space, agriculture, and forest. One possible reason for the confusion between different land uses is probably because of the large size of the study area. The area consists of three cities and unincorporated urban areas and thus includes a wide variety of different land-use structures. Moreover, some areas are characterized by distinct topographic variations that distort the spatial land-cover characteristics. Consequently, the metric/texture variability within the categories is fairly high, and causes some inaccuracies and confusion between the classes that might be distinct if only one city were investigated. Furthermore, the inaccuracies in the land-cover classification certainly propagate into the land-use classification and represent another source of error. Another more general issue that relates to the accuracy of the classification is the problem of representing a continuous variable in a categorized manner. For example, the boundaries between different densities of residential use are indistinct and cannot be perfectly described by a categorical variable (Knox, 1994). Spatial metrics and texture measurements describe the continuous nature of residential areas. This is reflected by the classification result where confusion happens among different types of residential land use. On the other hand, the continuous nature of texture parameters and spatial metrics may allow the description of the continuity of residential morphology and socio-economic and demographic characteristics. This offers a new avenue in describing and representing spatial urban form.

Figure 5 compares the classifications results using the spatial metrics, the texture parameters, and both measures. It shows that the combined application of both metrics and texture provides the highest classification. The spatial metrics, however, represent the most amount of information to separate between the land-use classes, with the KAPPA coefficient

TABLE 6.   ACCURACY ASSESSMENT OF THE FINAL LAND-USE MAP USING TEST AREAS

Class		Producer Accuracy	# of Samples	low_d 1	Med_d 2	high_d 3	multi 4	institut 5	recreat 6	com 7	Agri 8	forest 9
Low_dens_res	1	87.2	39	34	4	—	—	—	—	—	—	1
Med_dens_res	2	76.7	30	3	23	—	4	—	—	—	—	—
High_dens_res	3	78.0	41	—	3	32	5	—	—	1	—	—
Multi_unit_res	4	76.5	34	—	2	4	26	2	—	—	—	—
Institution	5	86.4	22	—	—	—	2	19	—	1	—	—
Recreation_open	6	73.9	23	1	—	—	—	—	17	1	4	—
Commerc_ind	7	74.4	43	—	1	1	5	4	—	32	—	—
Agri_rangl	8	62.2	45	1	1	—	—	2	7	—	28	6
Forest_wetland	9	78.6	28	—	—	—	—	—	2	—	4	22
Total			305	39	34	37	42	27	26	35	36	29
User Accuracy				87.2	67.6	86.5	61.9	70.4	65.4	91.4	77.8	75.9
Overall Accuracy (250/332) = 76.4%								**Kappa = 73.4%**				

Figure 5. Comparison of the classification results (producer and user accuracy) using the spatial metrics, the texture parameters, and the combination of the two. The accuracy values for the classification using both metrics and texture correspond to that in Table 6.
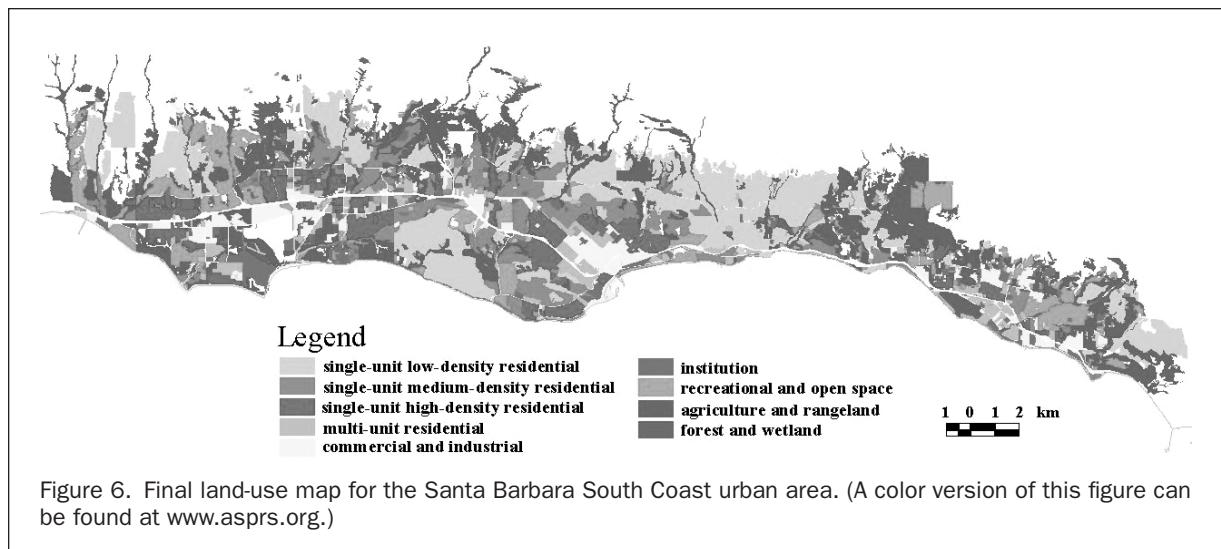
improving from 45.4 percent for texture-based classification, 63.7 percent for metric-based classification, and 73.4 percent for classification using metrics and texture. This result reflects the hierarchy of image interpretation elements (Figure 1), with the metrics providing a more complex level of information about size, shape, and pattern of land-cover elements. The superior performance of the metrics is especially obvious for the built-up categories (except for high-density residential) where the texture parameters add only minor additional information. For the class agriculture and rangeland, the texture parameters show a better accuracy than do metrics. This is related to the simple land-cover classification scheme used for the metric calculations that only considered buildings and green vegetation. Typical agricultural land-use patterns are not well reflected in this scheme, and the texture better represents this spatial feature of the landscape. This emphasizes that, although the texture parameters alone only provide an insufficient overall classification accuracy of about 51 percent, they add an important level of information that is not captured by the metrics.

Despite the described inaccuracies, the results of the land-use classification from the spatial metrics and the texture parameters are certainly encouraging and show that it is possible to capture several high-order interpretation elements known from visual image analysis (Figure 1) within a digital environment. The resulting final land-use map is presented in Figure 6. The map clearly represents forests and wetlands usually appearing as linear features of riparian areas. The downtown area of Santa Barbara is characterized by commercial use, which includes mixed commercial/residential uses. The closest surrounding ring indicates multi-unit residential and the next ring represents lower income areas of high density residential. Following this concentric concept, medium density residential builds the next ring and then high-income low density residential in the areas of Hope Ranch and Montecito that build the intermediate areas to the other urban centers of Goleta and Carpinteria. Goleta is a subsidiary center of Santa Barbara. This area is dominated by high-density residential areas that are clustered around the downtown core and other commercial areas. Agricultural areas are located near the cities of Goleta and Carpinteria. The major application of this land-use map is the incorporation into investigations of the UCIME project and related efforts in studying the spatial urban structure of the region and the integrated exploration of spatial planning support systems.

Figure 6. Final land-use map for the Santa Barbara South Coast urban area. (A color version of this figure can be found at www.asprs.org.)

Conclusions

In this study, we have examined the potential of using an object-oriented method to extract detailed urban land-use information from Ikonos imagery. An object-oriented approach was first applied to classify the land cover in the study area into three categories: building, vegetation, and the rest. Geometric information was then obtained from an additional source to aggregate land cover into land-use regions. Spatial metrics and image texture were calculated for each land-use region to describe its spatial characteristics. The Fisher linear discriminator was applied to classify the regions into nine land-use categories using the spatial metrics and texture measurements. The separability of different land uses was also examined, and the utility of each measurement has been evaluated and assessed.

Twenty-two spatial metrics and seven texture measurements were examined in the study. The results show that both spatial metrics and image texture contribute to the differentiation of nine urban land-use categories in the study area. For spatial metrics, metrics describing the spatial characteristics of vegetation patches seem to be most informative. Area coverage, the size and standard deviation (Mean patch size and standard deviation) as well as the spatial aggregation of the individual vegetation patches (Cohesion) provide most land-use discrimination. Building configuration is best characterized by area coverage, the regularity of the spatial arrangement (Nearest neighbor metrics), the dominance of one large building structure (Largest patch index), and the spatial heterogeneity of the individual building objects (Edge density). CONTAGION, as a measure of the overall spatial heterogeneity of a land-use region, provides another important land-use discriminator. The homogeneity has been identified as the most suitable texture measurement that makes an additional contribution to the differentiation of urban land uses.

The overall accuracy of land-use classification is 76.4 percent. This result is encouraging considering the level of classification detail and the large size of the study area. Spatial metrics contribute the most information to image classification, especially for separating built-up categories. The texture parameters alone do not result in sufficient classification accuracy, but they provide additional discriminating information that is not captured by spatial metrics. Most confusion in the classification appeared among different residential land-use types, and between the vegetation dominated classes such as recreation/open space, agriculture/rangeland, and forest/wetland. In general, the proposed approach can potentially provide a quantitative and consistent framework to identify urban land use structures. Considering the traditional air photointerpretation keys in identifying urban land-use categories (Bowden *et al.*, 1975; Haack *et al.*, 1997), this study indeed provides a bridge between the traditional approaches of visual image interpretation and the analysis of high-spatial-resolution satellite data. The spatial metrics and texture are able to represent higher-order image interpretation elements and capture the most important spatial characteristics that determine urban land-use categories. The quantitative nature of the metrics and textures make them comprehensive measurements to describe spatial urban morphology and structure with a potential for automating the process of identification and mapping of urban land-use classes. Further research should build on the results presented here and especially focus on the exploration of a more continuous representation of urban land-use configuration and its relationship to socio-economic and demographic characteristics, or environmental indicators. A general constraint of the study is the use of air-photo-derived land-use regions. The repeatable and transparent nature of the approach would be significantly improved if more automated land-use zone derivation algorithms would be used, an issue that will be addressed in further research.

References

Aplin, P., P. Atkinson, and P. Curran, 1999. Per-field classification of land use using the forthcoming very fine spatial resolution satellite sensors: Problems and potential solutions, *Advances in Remote Sensing and GIS Analysis* (P. Atkinson and N. Tate, editors), John Wiley and Sons, Chichester, United Kingdom, pp. 219–239.

Baatz, M., M. Heynen, P. Hofmann, I. Lingenfelder, M. Mimier, A. Schape, M. Weber, and G. Willhauck, 2001. *eCognition User Guide 2.0 : Object Oriented Image Analysis*, Definiens Imaging GmbH, Munich, Germany, 427 p.

Baraldi, A., and F. Parmiggiani, 1995. An investigation of the textural characteristics associated with gray level cooccurrence matrix statistical parameters, *IEEE Transactions on Geoscience and Remote Sensing*, 33(2):293–304.

Barnsley, M.J., and S.L. Barr, 1997. A graph based structural pattern recognition system to infer urban land-use from fine spatial resolution land-cover data, *Computers, Environment and Urban Systems*, 21(3/4):209–225.

———, 2000. Monitoring urban land use by Earth Observation, *Surveys in Geophysics*, 21:269–289.

Barnsley, M.J., S.L. Barr, A. Hamid, P.A.L. Muller, G.J. Sadler, and J.W. Shepherd, 1993. Analytical tools to monitor urban areas, *Geographical Information Handling—Research and Applications* (P.M. Mather, editor), John Wiley, Chichester, Sussex, United Kingdom, pp. 147–184.

Blaschke, T., and J. Strobl, 2001. What's wrong with pixels? Some recent developments interfacing remote sensing and GIS, *GeoBIT*, 6(6):12–17.

Bowden, L.W. (editor), 1975. Urban environments: inventory and analysis, *Manual of Remote Sensing, First Edition* (L.W. Bowden and E.L. Pruitt, editors), American Society of Photogrammetry, Falls Church, Virginia, pp. 1815–1880.

Couclelis, H., 1992. People manipulate objects (but cultivate fields): Beyond the raster-vector debate in GIS, *Theories and Methods of Spatio-Temporal Reasoning in Geographic Space* (A.U. Frank, I. Campari, and U. Formentini, editors), Lecture Notes in Computer Science, 639, Springer, Berlin, Germany, pp. 65–77.

Donnay, J.P., M.J. Barnsley, and P.A. Longley, 2001. Remote sensing and urban analysis, *Remote Sensing and Urban Analysis* (J.P. Donnay, M.J. Barnsley, and P.A. Longley, editors), Taylor and Francis, London, United Kingdom and New York, N.Y., pp. 3–18.

Estes, J.E., E.J. Hajic, and L.R. Tinney, 1983. Fundamentals of image analysis: Analysis of visible and thermal infrared data, *Manual of Remote Sensing, Second Edition* (Robert N. Colwell, editor), American Society of Photogrammetry, pp. 987–1124.

Gong, P., D.J. Marceau, and P.J. Howarth, 1992. A comparison of spatial feature extraction algorithms for land-use classification with SPOT HRV data, *Remote Sensing of Environment*, 40:137–151.

Gustafson, E.J., 1998. Quantifying landscape spatial pattern: What is the state of the art? *Ecosystems*, 1:143–156.

Haack, B.N., S.C. Guptill, R.K. Holz, S.M. Jampoler, J.R. Jensen, and R.A. Welch, 1997. Urban analysis and planning, *Manual of Photographic Interpretation, Second Edition* (W.R. Philipson, editor), American Society for Photogrammetry and Remote Sensing, Bethesda, Maryland, pp. 517–554.

Haralick, R., K. Shanmugam, and I. Dinstein, 1973. Texture features for image classification, *IEEE Transactions on Systems, Man, and Cybernetics*, SMC-3:610–621.

Herold, M., K.C. Clarke, and J. Scepan, 2002a. Remote sensing and landscape metrics to describe structures and changes in urban landuse, *Environment and Planning A*, 34:1443–1458.

Herold, M., A. Mueller, S. Guenter, and J. Scepan, 2002b. Object-oriented mapping and analysis of urban land use/cover using IKONOS data, *Geoinformation for European-Wide*

Integration—Proceedings of the 22nd EARSEL Symposium (T. Benes, editor), 04–06 June, Prague, Czech Republic (Millpress, Rotterdam, The Netherlands), pp. 531–538.

Herold, M., M. Gardner, and D. Roberts, 2003. Spectral resolution requirements for mapping urban areas, *IEEE Transactions on Geoscience and Remote Sensing*, in press.

Jensen, J.R., and D.C. Cowen, 1999. Remote sensing of urban/suburban infrastructure and socio-economic attributes, *Photogrammetric Engineering & Remote Sensing*, 65(5):611–622.

Johnsson, K., 1994. Segment-based land use classification from SPOT satellite data, *Photogrammetric Engineering & Remote Sensing*, 60(1):47–53.

Kailath. T., 1967. The divergence and Bhattacharyya distance measures in signal selection, *IEEE Transactions on Communication Theory*, 15:152–160.

Klecka, W.R., 1980. *Discriminant Analysis*, Sage Publications, London, United Kingdom, 71 p.

Knox, P.L., 1994. *Urbanization: Introduction to Urban Geography*, Prentice Hall, New Jersey, 436 p.

Landgrebe, D.A., and L. Biehl, 2001. *An Introduction to MultiSpec*, Purdue University, West Lafayette, Indiana, URL: http://www.ece.purdue.edu/~biehl/MultiSpec/last accessed September 2002.

Liu, X., and K.C. Clarke, 2002. Estimation of residential population using high resolution satellite imagery, *Proceedings of the 3rd Symposium on Remote Sensing of Urban Areas* (D. Maktav, C. Juergens, and F. Sunar-Erbek, editors), 11–13 June, Istanbul, Turkey (Istanbul Technical University), pp. 153–160.

Mausel, P.W., W.J. Kramber, and J.K. Lee, 1990. Optimum band selection for supervised classification of multispectral data, *Photogrammetric Engineering & Remote Sensing*, 56:55–60.

McGarigal, K., S.A. Cushman, M.C. Neel, and E. Ene, 2002. *FRAGSTATS: Spatial Pattern Analysis Program for Categorical Maps*, University of Massachusetts, Amherst, Massachusetts, URL: www.umass.edu/landeco/research/fragstats/fragstats.html, last accessed September 2002.

McKeown, D.M., 1988. Building knowledge-based systems for detecting man-made structures from remotely-sensed imagery, *Philosophical Transactions of the Royal Society London*, *Series A*, 324:423–435.

Moller-Jensen, L., 1990. Knowledge-based classification of an urban area using texture and context information in Landsat TM imagery, *Photogrammetric Engineering & Remote Sensing*, 56(6):899–904.

O'Neill, R.V., J.R. Krummel, R.H. Gardner, G. Sugihara, B. Jackson, D.L. Deangelis, B.T. Milne, M.G. Turner, B. Zygmunt, S.W. Christensen, V.H. Dale, and R.L. Graham, 1988. Indices of landscape pattern, *Landscape Ecology*, 1:153–162.

Peplies, R.W., 1974. Regional analysis and remote sensing: A methodological approach, *Remote Sensing: Techniques for Environmental Analysis* (J.E. Estes and L.W. Senger, editors), Hamilton Publishing Company, Santa Barbara, California, pp. 277–291.

Small, C., 2001. Scaling properties of urban reflectance spectra, *Proceedings of AVIRIS Earth Science and Applications Workshop*, 27 February—02 March, Palo Alto, California, (NASA) Jet Propulsion Laboratory, Pasedena, California, URL: http://popo.jpl.nasa.gov/docs/workshops/01_docs/2001Small_web.pdf, last accessed September 2002.

UCIME, 2001. *Urban Change—Integrated Modeling Environment*, University of California, Santa Barbara, URL: http://www.geog.ucsb.edu/~kclarke/ucime/index.html, last accessed December 2002.

Webster, C.J., 1995. Urban morphological fingerprints, *Environment and Planning B*, 22:279–297.

Welch, R., 1982. Spatial resolution requirements for urban studies, *International Journal of Remote Sensing*, 3(2):139–146.

Zhan, Q., M. Molenaar, and K. Tempfli, 2002. Hierarchical image object based structural analysis toward urban land use classification using HR imagery and airborne lidar data, *Proceedings of the 3rd Symposium on Remote Sensing of Urban Areas* (D. Maktav, C. Juergens, and F. Sunar-Erbek, editors), 11–13 June, Istanbul, Turkey (Istanbul Technical University), pp. 251–258.